Efficient in Situ One-Pot Synthesis of Water-Soluble Hydroxynaphthoquinones for Redox Flow Batteries

Patricia Bassil, Didier Floner, Solène Guiheneuf, Ludovic Paquin, Florence Geneste

Efficient *In Situ* One-Pot Synthesis of Water-Soluble Hydroxynaphthoquinones for Redox Flow Batteries

Patricia Bassil, Didier Floner*, Solène Guiheneuf, Ludovic Paquin, Florence Geneste*

Univ Rennes, CNRS, ISCR, UMR 6226, F-35000 Rennes, France

Florence.geneste@univ-rennes.fr, didier.floner@univ-rennes.fr

Abstract

Given the importance of energy storage and its hybridization with renewable technologies for the energy transition, the development of redox flow batteries (RFB) is receiving particular attention. Among the various emerging technologies, aqueous organic redox flow batteries (AORFBs) are of particular interest, as the objectives in terms of durability, cost and safety can be achieved thanks to the possibilities offered by molecular engineering. While anthraquinones have been widely explored as negolyte, few works report the use of naphthoquinones. This work aims to exploit an innovative *in situ* and cost-effective method for the one-pot synthesis of water-soluble naphthoquinones for application as negolyte in redox flow batteries. As exemplified with alizarin, the energy of the naphthoquinone synthetic reaction in fuel cell mode can be recovered and the electrolyte solution used directly in redox flow batteries without purification. A 0.3 M naphthoquinone solution paired with 0.6 M ferrocyanide demonstrated

good stability compared with other naphthoquinones with a capacity fade rate of 0.017%/cycle (0.84%/day) over 320 cycles. Additionally, the system exhibited one of the highest energy efficiency (82%) and a power density of 162 mW cm^{-2} at 50% SOC. These first results are promising for further exploration of new water-soluble naphthoquinones efficiently synthesized from hydroxyanthraquinones for application in AORFBs.

Keywords: naphthoquinone, redox flow battery, one-pot synthesis, energy recovery, hydroxyanthraquinones

1. Introduction

The development of renewable energies such as wind power and solar photovoltaics requires efficient, low-cost and scalable stationary energy storage systems. Redox flow battery technology is promising as it is simple, with a flexible design enabling decoupling of power (Watt) and energy (Watt-hour) and offers reliable long-term performance. Aqueous organic redox flow batteries (AORFBs) have been widely studied since they have many advantages.[1-5] First, molecular engineering uses organic elements that are abundant on earth, and offers enormous potential for improving performance in terms of safety, cost, solubility, redox potential, kinetics and stability. Second, despite its limited electrochemical potential window (1.2 V), water is a very efficient solvent for solubilizing ions, resulting in a highly conductive electrolyte, and is cheap and extremely safe. Among organic molecules that are electroactive in aqueous media, quinones have been extensively studied,[2, 6, 7] due to their molecular diversity and the possibility of using them in acidic, neutral and basic media. Alkaline solutions are of particular interest, as in these media the non-toxic, low-cost ferri/ferrocyanide redox couple can be used as posolyte.[8-10]

While substituted anthraquinones have been extensively studied for their high stability,[7] few studies have focused on the use of naphthoquinones as negolytes in aqueous redox flow batteries, due to their limited solubility in water and high redox potential.[11-19] The most studied naphthoquinone in AORFB is 2-hydroxy-1,4-naphthoquinone, known as "lawsone", which is a naturally abundant moderate-cost red-orange pigment.[11] It could be used in an alkaline medium at a concentration of 0.5 M paired with 4-OH-TEMPO with a theoretical cell voltage of 1.30 V.[13] Unfortunately, it exhibits chemical instability during cycling, probably due to a Michael addition on the alpha-carbon of the hydroxyl group.[17] For this reason, studies have focused on dimers blocking this position (bislawsone).[17] When paired with $K_4Fe(CN)_6$, bislawsone could be cycled in a battery with a concentration of 1 M. However, its reduced form undergoes tautomerization, leading to an inactive quinone and thus losing its electrochemical activity.[15] It degrades during cycling to lawsone, but leads to greater solubility of redox compounds in solution (1.26 M in 1 M KOH). The authors showed that the increase in solubility was due to the presence of sulfite ions, which also improved lawsone stability.[14] Another water-soluble naphthoquinone tested in AORFB is 2-hydroxy-3-carboxy-1,4-naphthoquinone[18], synthesized in two steps from low-cost commercial reagents. It exhibits a solubility of 1.2 M and achieves a cell voltage of 1.02 V when coupled with $K_4Fe(CN)_6$.[18] While it could be cycled in a 0.1 M battery with a capacity loss of 3.4% per day for 100 cycles, the authors observed instability in its reduced form.

The low-cost synthesis of a stable, water-soluble naphthoquinone with a redox potential suitable for application in redox flow batteries thus appears to be challenging. This work reports the synthesis and implementation in AORFB of a water-soluble naphthoquinone substituted by a carboxylate pendant arm using an innovative, one-step synthesis approach from alizarin, a low-cost commercial pigment. Paired with potassium ferrocyanide, a cell voltage of 0.93 V was achieved. Interestingly, the synthesis is performed directly in the battery cell with the electrolyte

medium for AORFB for both electrolytes, avoiding laborious purification procedures. Furthermore, it enables the recovery of energy consumed during the reaction in the form of electric current, as the synthesis can be performed in a fuel cell mode. Finally, this synthetic method makes it possible to use hard-to-isolate naphthoquinones, which are not very stable in acidic media, in AORFB. It can also be extended to other hydroxylated anthraquinones.

2. Experimental section

2.1. Electrochemical analyses

Electrochemical analyses were carried out in a three-electrode cell with a Biologic SP150 potentiostat controlled by EC-lab® software. A gold electrode (3.14×10^{-2} cm^2), a platinum counter electrode and a saturated KCl/Ag/AgCl reference electrode were used. Linear voltammetry was performed on a rotating gold Orygalys electrode (3.14×10^{-2} cm^2).

2.2. Solubility measurements

The solubility of 4-(3-hydroxy-1-methylene-4-oxo-1,4-dihydronaphthalen-2-yl)-2-oxobut-3-enoic acid (**2,3-HButCNQ**) was measured by adding it to a 1 M KOH solution until no further solid could be dissolved. The suspension was filtered through a 0.45 μm nylon syringe filter. The saturated solution was then diluted with 1 M KOH solution, and the concentration was assessed by UV-Vis spectroscopy (Agilent Cary 60 UV-Vis spectrophotometer). The concentration was calculated according to a calibration curve performed at pH 14 (Figure S3). The resulting solubility value for the oxidized form was 0.33 M.

2.3. Alizarin oxidation in a flow electrochemical cell

Alizarin oxidation was carried out under argon in a homemade electrochemical flow cell.[20] The working electrode was a graphite felt (Recycled Vein Graphite RVG 4000 supplied by Mersen, France, 48 mm in diameter and 12 mm thickness), with a saturated KCl/Ag/AgCl reference

electrode implanted in the middle of the graphite felt. The working and counter electrodes were separated by a cation exchange membrane (Ionac 3470 - Lanxess SAS, Courbevoie, France). Chronoamperometry was controlled by a VersaSTAT 3 workstation (Princeton Applied Research). Argon-degassed alizarin solution percolated the electrode and was recycled by a Gilson peristaltic pump (Middleton, WI. USA). The reaction was followed by cyclic voltammetry on a glassy carbon electrode (0.125 cm^2).

2.4. Alizarin oxidation in fuel cell mode

Alizarin oxidation was carried out in a cell developed by the KEMIWATT company (France), containing two 4.6 mm-thick SGL Carbon graphite electrodes with an active surface area of 25 cm^2, graphite current collectors and a 50 μm Nafion cation exchange membrane. A cell voltage of 0.2 V between ferricyanide (III) and alizarin was applied until the current dropped to -35 mA. The electrolyte solutions were 250 mL of 0.1 M alizarin in 1 M KOH and 1000 mL of 0.2 M potassium ferricyanide (III) in 0.3 M KOH. The structure of the main product **2,3-HButCNQ** was determined from NMR analyses (Figure S1) and mass spectrometry.

^{1}H NMR (MeOD-d4, 268 K, 500 MHz): δH (ppm): 8.30 (1H, d, J_{trans} = 16.1 Hz, H_4), 8.08 (1H, dd, ^{3}J = 7.7 Hz, ^{4}J = 1.2 Hz, H_{11}), 7.97 (1H, dd, ^{3}J = 7.4 Hz, ^{4}J = 1.2 Hz, H_{14}), 7.72 (1H, td, ^{3}J = 7.4 Hz, ^{4}J = 1.2 Hz, H_{12}), 7.69 (1H, d, J_{trans} = 16 Hz, H_3), 7.61 (1H, td, ^{3}J = 7.4 Hz, ^{4}J = 1.2 Hz, H_{13}).

HSQC-edited and HMBC NMR (MeOD-d4, 268 K, 500 MHz): δc (ppm) : 201.47 (C_2), 186.75 (C_7), 184.67 (C_{10}), 176.41 (C_6), 175.68 (C_1), 146.64 (C_4), 137.76 (C_9), 136.26 (C_{12}), 134.15 (C_8), 133.48 (C_{13}), 128.17 (C_{11}), 127.91 (C_{14}), 120.98 (C_3), 116.52 (C_5).

ESI-MS: m/z = 271 [M-H] for $C_{14}H_8O_6$

2.5. Redox flow battery experiments

Redox flow battery experiments were carried out in a cell developed by the KEMIWATT company (France), containing two 4.6 mm thickness SGL Carbon graphite electrodes with an active surface area of 25 cm^2, graphite current collectors and a 50 μm Nafion cation exchange membrane. The positive and negative electrolytes flowed at a rate of 50 mL min^{-1} through KNF pumps.

For experiments performed with around 0.08 M naphthoquinone, the solutions obtained from alizarin oxidation were used directly in the battery.

For experiments performed with 0.3 M naphthoquinone, an 80 mL solution of the oxidized alizarin was concentrated to a volume of 20 mL. An equimolar solution of $K_4Fe(CN)_6$ and $Na_4Fe(CN)_6$ (0.6 M) in 1 M KOH (25 mL) was used as posolyte. A slight excess of ferrocyanide was used due to the commonly admitted degradation of ferrocyanide in strong basic medium[7] and a mixture of K^+ and Na^+ salts for solubility improvement.[21]

The negolyte was purged with argon for 10 min, before the battery experiments, and the posolyte reservoir was covered by aluminum foil to protect it from light.

3. Results and discussion

3.1. Electrosynthesis of the substituted naphthoquinone from alizarin

Cyclic voltammetry analysis of alizarin in a strong basic medium shows two oxidation peaks at -0.01 V *vs* Ag/AgCl and 0.15 V *vs* Ag/AgCl, leading to the apparition of two new reversible systems at -0.77 V *vs* Ag/AgCl and -0.28 V *vs* Ag/AgCl (Figure 1a).

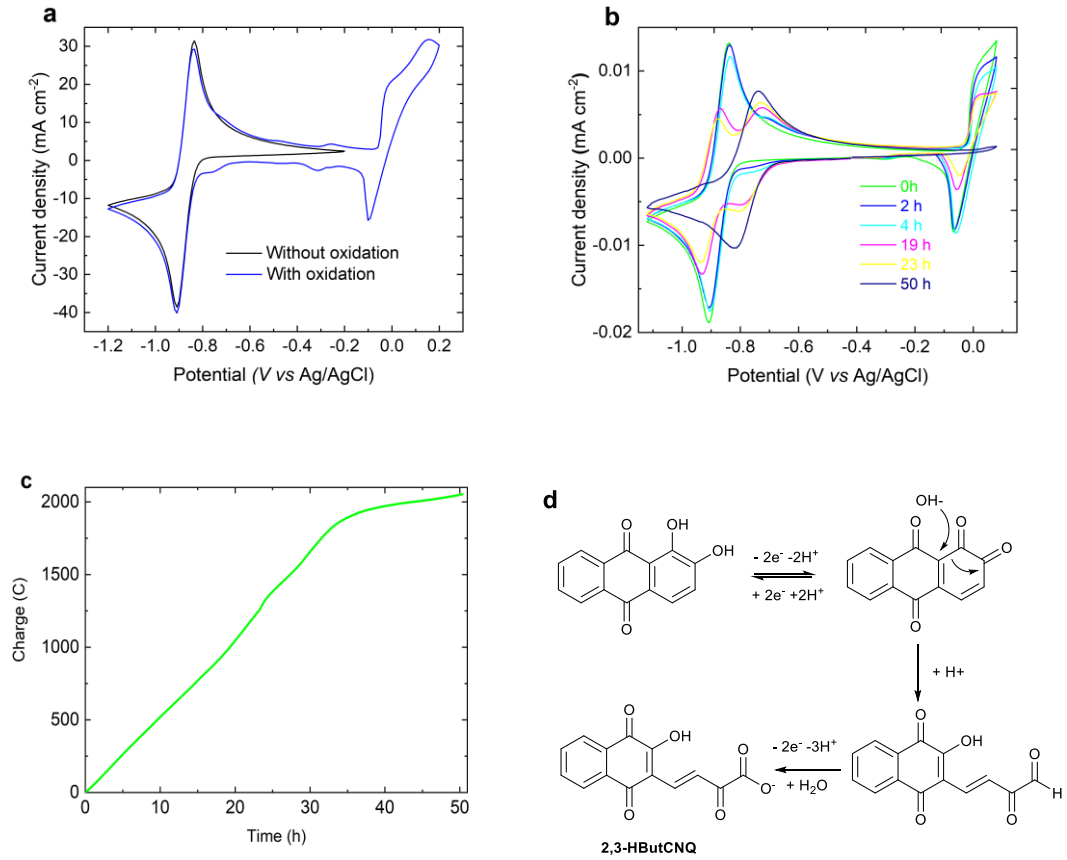

Figure 1. Electrosynthesis of naphthoquinone **2,3-HButCNQ (a)** Cyclic voltammograms of 0.1 M alizarin in 1 M KOH at 0.1 V s^{-1} (**b)** *Operando* cyclic voltammetry analysis (**c)** Coulometry during potentiostatic oxidation at -0.05 V *vs* Ag/AgCl of 0.1 M alizarin in 1 M KOH (**d)** Proposed mechanism for the oxidation of alizarin into naphthoquinone **2,3-HButCNQ** (**e**)

To determine the nature of the species formed after oxidation, 0.1 M alizarin in 1 M KOH was electrolyzed at -0.05 V *vs* Ag/AgCl under argon in a flow electrochemical cell[20] on a graphite felt electrode. *Operando* analysis by cyclic voltammetry was used to monitor the reaction progress (Figure 1b).

During electrolysis, alizarin was oxidized, leading to a decrease in the current intensity of its peaks in favor of the new reversible system at -0.77 V vs Ag/AgCl. After 50h of electrolysis, alizarin was totally oxidized and no more oxidation peak was observed. The total charge passed to oxidize alizarin was around 2000 C (Figure 1c).

To identify the oxidation products, the solution was acidified with HCl, resulting in the precipitation of a compound that exhibited the reversible system at -0.77 V vs Ag/AgCl in cyclic voltammetry. This solid was isolated and characterized by NMR (Figure S1) and mass spectrometry. As depicted in Figure 1d, the structure of the isolated compound corresponded to the naphthoquinone (4-(3-hydroxy-1-methylene-4-oxo-1,4-dihydronaphthalen-2-yl)-2-oxobut-3-enoic acid) **(2,3-HButCNQ)**, containing a carboxylate pendant arm.

A proposed mechanism involves the oxidation of the catechol into the corresponding quinone, followed by a 1,8-Michael addition of OH^- leading to ring opening and further oxidation of the aldehyde into carboxylate (Figure 1d). This 4-electron oxidation process was not supported by the total charge passed during the electrolysis, corresponding to about 6-electron oxidation. However, according to cyclic voltammetry analysis (Figure 1b), the current intensity of the 2-electron wave of **2,3-HButCNQ** after electrolysis corresponded to about 2/3 of that of alizarin, indicating that the reaction was not quantitative even if **2,3-HButCNQ** was the major product. This result was confirmed by ^{1}H-NMR analysis of the crude medium after oxidation of alizarin and evaporation of water, which showed the presence of several products (Figure S2). Coulometry experiments conducted with other hydroxylated anthraquinone, alizarin RedS and purpurin (Table S1), exhibited a 4-electron oxidation reaction. This aligns with the mechanism proposed in Figure 1d and is promising for future work on the synthesis of new naphthoquinone derivatives from these two commercially available anthraquinones.

3.2. Physico-chemical characterizations of naphthoquinone 2,3-HButCNQ

The solubility of naphthoquinone **2,3-HButCNQ** in 1 M KOH, determined by UV-Visible spectrometry (Figure S3) was 0.33 M, corresponding to an energy density of 19.3 Wh L^{-1}. It is therefore more soluble than alizarin in 1 mM KOH (0.23 M), probably due to the presence of the carboxylate group.

The reduction potential showed a pH-dependent behaviour. The slopes in Pourbaix diagram (Figure S4) is close to −30 mV pH^{-1}, indicating a one-proton two-electron process. Transient voltammetric techniques were applied to quantify the diffusivity of **2,3-HButCNQ**. The linear correlation of $Ip = f(\sqrt{\nu})$ allows us to estimate the diffusion coefficient of this molecule (Figure S4), which was found to be 4.86×10^{-6} cm^2 s^{-1}. Then, the apparent rate constant k^0 was determined by linear voltammetry performed on a rotating disk electrode at different rotation speeds using the Koutecky-Levich method (Figure S4). Construction of the Tafel graph, η as a function of $\log i_K$, enables k^0 to be calculated from the intercept of the linear regression line with the x-axis, which is equal to $\log(nFAk^0C)$. From the experimental data, the extrapolated value of k^0 was 11.30×10^{-3} cm s^{-1}.

The diffusion coefficient and apparent electron transfer rate constants are of the same order of magnitude as the hydroxyanthraquinones used in AORFB,[22] with one of the best reported k^0 values.[13, 18]

3.3. Synthesis of the naphthoquinone 2,3-HButCNQ in a redox flow battery in fuel cell mode

Since alizarin can be oxidized at a relatively low potential, we expected that it could be spontaneously oxidized by ferricyanide, usually used as posolyte in alkaline AORFB. To test the synthesis of the naphthoquinone **2,3-HButCNQ** in fuel cell mode (using alizarin as fuel and ferricyanide (III) as oxidant), a solution of 0.1 M alizarin was prepared in 1 M KOH as anolyte and a solution of 0.2 M potassium ferricyanide in 0.3 M KOH was used as catholyte, with a volume ratio corresponding to a large excess of oxidant. The fuel cell was operated under a potentiostatic mode with an applied cell voltage of 200 mV. The initial current was 2.3 A and the oxidation was stopped when it reached 35 mA (Figure 2a). A high capacity of 4.1 A h was

obtained due to the exchange of 6 electrons (Figure 2b). The evolution of the electrical power produced by the cell is shown in Figure 2c. The initial power of the cell was 420 mW, corresponding to an initial power density of 17 mW cm^{-2}.

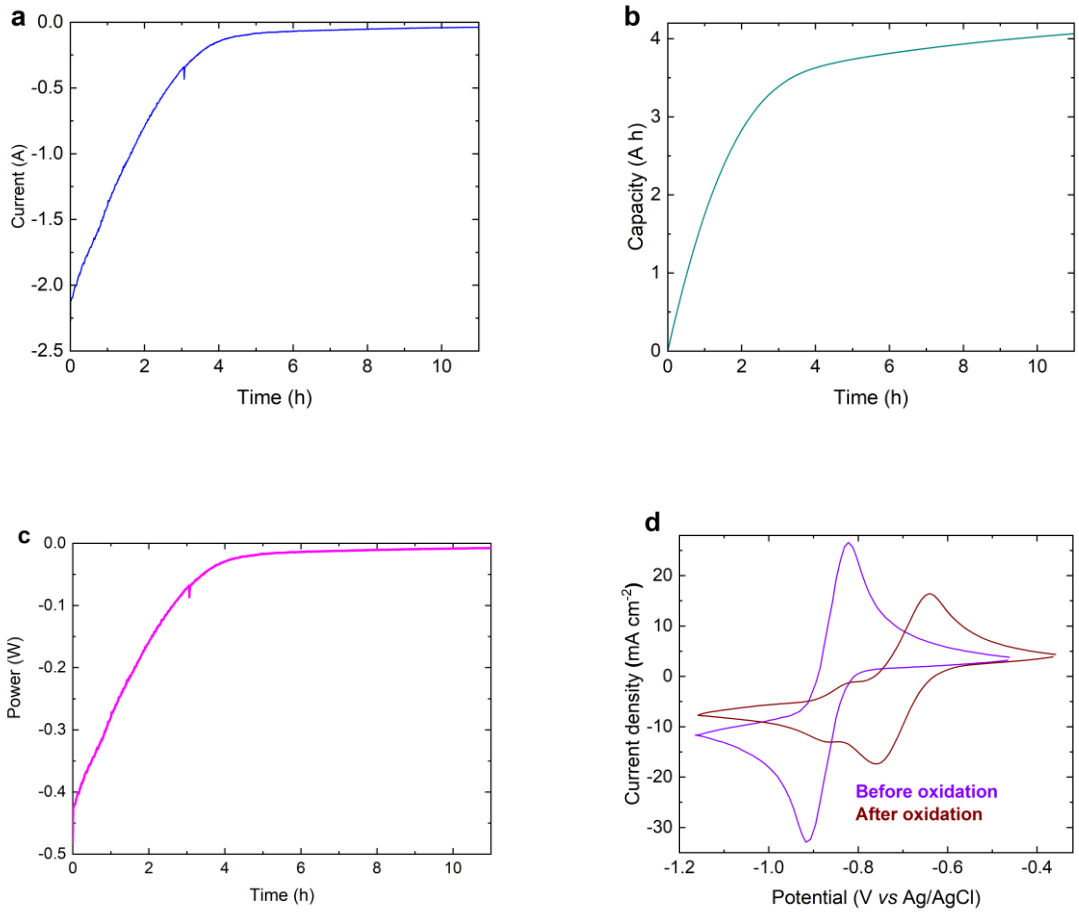

Figure 2. (a) Current, (**b)** capacity and (**c)** power *vs* time evolution during alizarin oxidation in a fuel cell mode (using 0.1 M alizarin in 1 M KOH as anolyte and 0.2 M potassium ferricyanide in 0.3 M KOH as catholyte) (**d)** Cyclic voltammograms of the anolyte solution before and after the oxidation in fuel cell mode on gold electrode. Scan rate: 0.1 V s^{-1}

After 10h of electrolysis, cyclic voltammetry analysis revealed an alizarin oxidation around 80% (Figure 2d). These first experiments demonstrated the feasibility of *in situ* synthesis of the naphthoquinone **2,3-HButCNQ**, thereby enabling energy recovery from the oxidation reaction.

Furthermore, total oxidation of alizarin into **2,3-HButCNQ** is not necessary for AORFB application since alizarin is a reversible system with a potential close to that of **2,3-HButCNQ** and will be diluted in the solution, preventing solubility issues.

3.4. Coupling of *in situ* synthesis of 2,3-HButCNQ with its implementation in AORFB

To check the possibility of directly using the electrolyte solutions obtained after the *in situ* oxidation of alizarin in AORFB, 25 mL of each electrolyte from the synthesis in fuel cell mode were implemented in a flow battery and cycled in galvanostatic mode with a current density of 20 mA cm^{-2}. The capacity *vs* cycle number is given in Figure 3a and the corresponding charge-discharge curves in Figure S5a. Remarkably, after 700 cycles, the capacity fade rate was found to be 0.020%/cycle (1.32 %/day), which is in the same order of magnitude as the best values obtained in literature with hydroxyanthraquinones[22] and other naphthoquinones (Table 1).

Table 1. Performance of naphthoquinones as negolyte in AORFB

Naphthoquinones	**Cycle number (Conc. in M)**	**Capacity fading %/cycle (%/day)**	**EE (%)**	**Max power density (mW cm^{-2}) (SOC)**	**References**
2,3-HCNQ	50 (0.5) 20 (1)	0.053 (3.4) 1.8 (6.4)	68.8	200 (50)	[18]
Lawsone	215 (0.1)	0.0079 (-)	75	-	[13]
Bislawsone	260 (0.1) 400 (0.5)	0.008 (0.55) 0.038 (0.74)	77 79.3	150 (50) 250 (50)	[17]
NQ-S + Lawsone	80 (1.2) 200 (0.6)	0.258 (-) 0.027 (-)	- 55	- 90	[15]
Lawsone (with sulfite)	100 (0.4)	0.091 (-)	57	-	[14]
2,3-HButCNQ	730 (~0.08) 350 (0.3)	0.020 (1.32) 0.017 (0.84)	86 82	80-105 (50) 85-110 (50)	This work

2,3-HCNQ (2-hydroxy-3-carboxy-1,4-naphthoquinone), **Lawsone** (2-hydroxy-1,4-naphthoquinone), **NQ-S** (1,2-naphthoquinone-4-sulfonic acid sodium salt), **2,3-HButCNQ** (4-(3-hydroxy-1-methylene-4-oxo-1,4-dihydronaphthalen-2-yl)-2-oxobut-3-enoic acid)

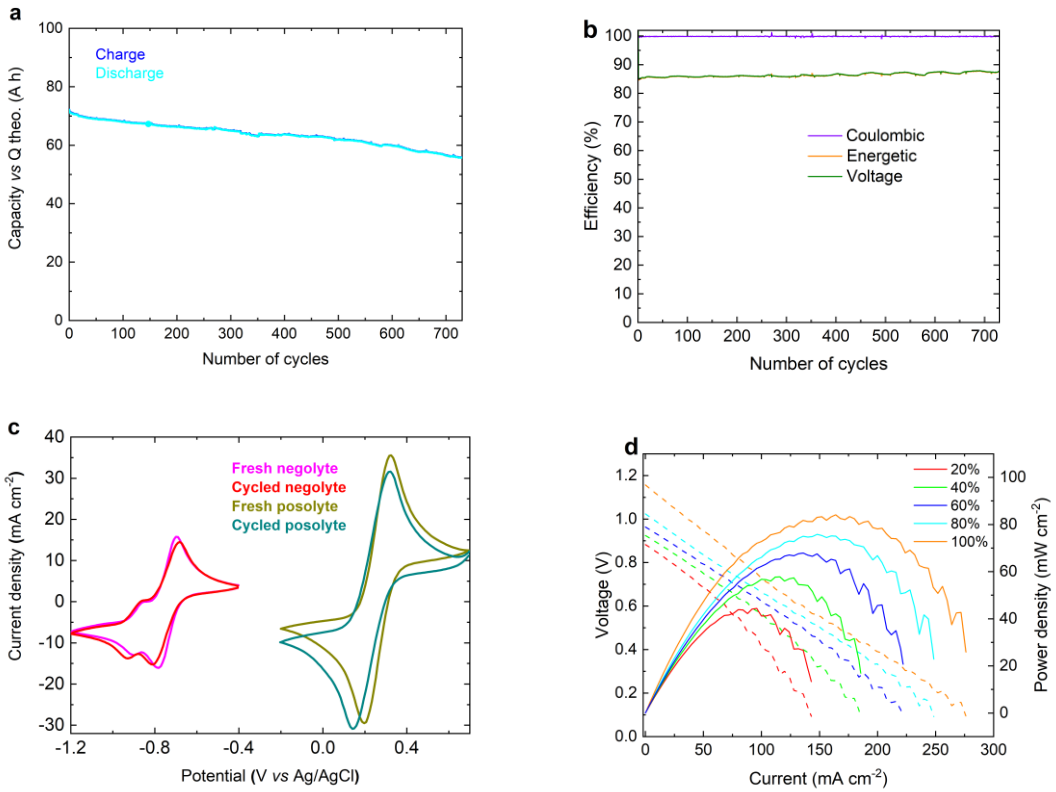

Figure 3. (**a)** Evolution of the capacity with time according to the cycle numbers (20 mA cm^{-2}; cut-off voltages 0.4 and 1.35 V) (**b)** Coulombic efficiency (CE), voltage efficiency (VE) and round-trip energy efficiency (EE) (**c)** Cyclic voltammograms of negolyte before and after 730 cycles. Scan rate: 0.1 V s^{-1} **(d)** Power density *versus* current density at 20, 40, 60, 80 and 100% SOC.

The coulombic efficiency (Figure 3b) of this battery was 99.8%, and the energy efficiency was 86%, which is comparable with anthraquinones[22] and higher than the values previously reported for other naphthoquinones (Table 1).

The stability of the redox compounds after cycling was checked by cyclic voltammetry (Figure 3c). A variation of around 7-8% was observed between the peak surface area before and after cycling. This value is half the capacity fade rate of 0.020%/cycle, which corresponds to a loss of 15% after 730 cycles. The difference may be attributed to water transfer since the cycling is performed in galvanostatic mode with a constant cut-off voltage in charge and/or to oxygen leakage. Cyclic voltammetry analysis (Figure S6) did not show the presence of naphthoquinone

in the posolyte compartment, showing that the crossover of **2,3-HButCNQ** was not responsible for the capacity decrease.

The polarization curves (Figure 3d) were performed at 20, 40, 60 and 100% state of charge. A peak galvanic power density of 83 mW cm^{-2} was obtained at 100% SOC. However, the area specific resistance (ASR) measured at 50% SOC[23] fluctuates between 2.5 and 1.8 Ω cm^2 (Figure S7). The decrease in resistance could be attributed to membrane activation during cycling since no preliminary treatment was performed. The power density calculated from ASR[23] evolved, as expected, in the opposite direction to the resistance, ranging from 80 to 105 mW cm^{-2}.

The naphthoquinone was also evaluated in AORFB at a higher concentration (Figure 4 and Figure S5b). The solution of naphthoquinone **2,3-HButCNQ** prepared according to the fuel cell mode was concentrated to reach a concentration close to 0.3 M and then implemented in an AORFB with a 0.6 M solution of potassium and sodium ferrocyanide.

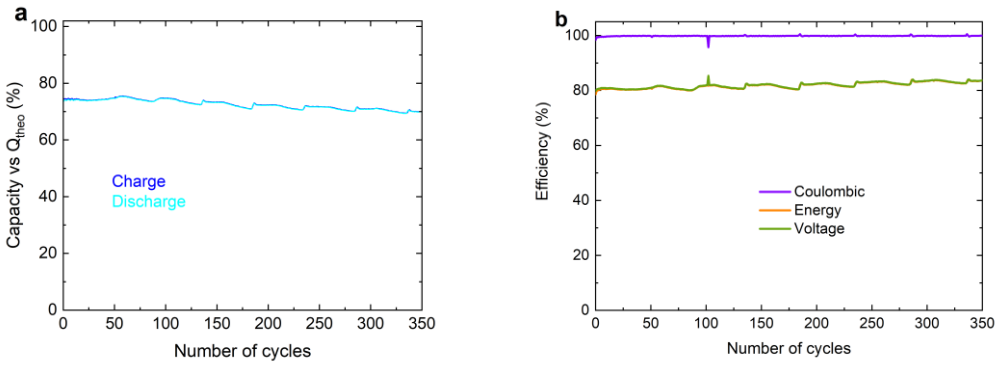

Figure 4 (**a)** Evolution of the capacity with time according to the cycle numbers (40 mA cm^{-2}; cut-off voltages 0.4 and 1.35 V) (**b)** Coulombic efficiency (CE), voltage efficiency (VE) and round-trip energy efficiency (EE)

The capacity fade rate of **2,3-HButCNQ** was 0.017 %/cycle (0.84%/day), which is close to the value found for the battery performed at a lower concentration. It is interesting to note that the stability was not affected by increasing the concentration of **2,3-HButCNQ** in negolyte

contrary to what had been observed with other naphthoquinone derivatives (Table 1). The coulombic efficiency was 99.8% and the energy efficiency was 82%, which is similar to experiments performed with 0.08 M naphthoquinone. The energy density of the battery in operation was around 13 Wh L^{-1}, considering only the negolyte compartment and 5.8 Wh L^{-1} if both compartments were taken into account.

It should be noted that alizarin can be added in small solid portions during naphthoquinone synthesis in fuel cell mode to finally obtain a ready-to-use solution of **2,3-HButCNQ** as negolyte for AORFB application (Figure S8).

4. Conclusions

This work highlights an original process for the *in situ* one-step synthesis of naphthoquinones from commercially available hydroxyanthraquinones. This synthesis, involving spontaneous redox reactions, can be carried out in a fuel cell mode, allowing for the recovery of reaction energy and direct utilization of both posolyte and negolyte solutions in AORFB applications. This avoids the necessity to purify compounds that are highly stable in basic media but difficult to isolate due to their relative instability in acidic media. This method was exemplified using alizarin, a relatively low-cost commercial pigment. The negolyte solution containing the *in situ* synthesized 0.3 M naphthoquinone paired with ferrocyanide as posolyte led to a good capacity retention of 0.017%/cycle (0.84%/day). Moreover, it showed high energy efficiency, comparable to anthraquinones, and a power density of 162 mW cm^{-2} at 50% SOC. This energy-effective *in situ* synthesis can be extended to other hydroxyanthraquinones such as purpurin and alizarin RedS to synthesize new stable and soluble hydroxynaphthoquinones in an alkaline medium. This advancement contributes significantly to AORFB, meeting the cost, performance and stability targets required to become attractive for intermittent energy storage applications.

Supporting Information

NMR spectra, UV-vis calibration curve, electrochemical characterizations, battery experiments. Figures S1 to S8 and Table S1.

Acknowledgements

This work was supported by a French government grant managed by the Agence Nationale de la Recherche under the France 2030 program (ANR-23-PEBA-0001) and by an Eiffel grant from the French Ministry of Foreign Affairs (PB). We thank A. Bondon for his help with the NMR analyses.

References

(1) Chen, R., Redox flow batteries for energy storage: Recent advances in using organic active materials. *Curr. Opin. Electrochem.* **2020,** *21*, 40-45.

(2) Liu, Y.; Chen, Q.; Sun, P.; Li, Y.; Yang, Z.; Xu, T., Organic electrolytes for aqueous organic flow batteries. *Mater. Today Energy* **2021,** *20*, 100634.

(3) Luo, J.; Hu, B.; Hu, M.; Zhao, Y.; Liu, T. L., Status and prospects of organic redox flow batteries toward sustainable energy storage. *ACS Energy Lett.* **2019,** *4* (9), 2220-2240.

(4) Singh, V.; Kim, S.; Kang, J.; Byon, H. R., Aqueous organic redox flow batteries. *Nano Res.* **2019,** *12*, 1988-2001.

(5) Zhong, F.; Yang, M.; Ding, M.; Jia, C., Organic electroactive molecule-based electrolytes for redox flow batteries: status and challenges of molecular design. *Front. Chem.* **2020,** *8*, 451.

(6) Symons, P., Quinones for redox flow batteries. *Curr. Opin. Electrochem.* **2021,** *29*, 100759.

(7) Fontmorin, J.-M.; Guiheneuf, S.; Godet-Bar, T.; Floner, D.; Geneste, F., How anthraquinones can enable aqueous organic redox flow batteries to meet the needs of industrialization. *J. Colloid Interface Sci.* **2022**, 101624.

(8) Lin, K.; Chen, Q.; Gerhardt, M. R.; Tong, L.; Kim, S. B.; Eisenach, L.; Valle, A. W.; Hardee, D.; Gordon, R. G.; Aziz, M. J., Alkaline quinone flow battery. *Science* **2015,** *349* (6255), 1529-1532.

(9) Lê, A.; Floner, D.; Roisnel, T.; Cador, O.; Chancelier, L.; Geneste, F., Highly soluble Fe (III)-triethanolamine complex relevant for redox flow batteries. *Electrochim. Acta* **2019,** *301*, 472-477.

(10) Fontmorin, J.-M.; Guiheneuf, S.; Bassil, P.; Geneste, F.; Floner, D., Addition of weak acids in electrolytes to prevent osmosis in aqueous organic redox flow batteries. *Electrochem. Commun.* **2021,** *132*, 107148.

(11) Ding, Y.; Li, Y.; Yu, G., Exploring Bio-inspired Quinone-Based Organic Redox Flow Batteries: A Combined Experimental and Computational Study. *Chem* **2016,** *1* (5), 790-801.

(12) Er, S.; Suh, C.; Marshak, M. P.; Aspuru-Guzik, A., Computational design of molecules for an all-quinone redox flow battery. *Chem Sci* **2015,** *6* (2), 885-893.

(13) Hu, P.; Lan, H.; Wang, X.; Yang, Y.; Liu, X.; Wang, H.; Guo, L., Renewable-lawsone-based sustainable and high-voltage aqueous flow battery. *Energy Storage Mater.* **2019,** *19*, 62-68.

(14) Lee, W.; In Shim, K.; Park, G.; Han, J. W.; Kwon, Y., Rational design of composite supporting electrolyte required for achieving high performance aqueous organic redox flow battery. *Chem. Eng. J.* **2023,** *464*, 142661.

(15) Lee, W.; Park, G.; Kwon, Y., Alkaline aqueous organic redox flow batteries of high energy and power densities using mixed naphthoquinone derivatives. *Chem. Eng. J.* **2020,** *386*, 123985.

(16) Schwan, S.; Schroder, D.; Wegner, H. A.; Janek, J.; Mollenhauer, D., Substituent Pattern Effects on the Redox Potentials of Quinone-Based Active Materials for Aqueous Redox Flow Batteries. *ChemSusChem* **2020,** *13* (20), 5480-5488.

(17) Tong, L.; Goulet, M.-A.; Tabor, D. P.; Kerr, E. F.; De Porcellinis, D.; Fell, E. M.; Aspuru-Guzik, A. n.; Gordon, R. G.; Aziz, M. J., Molecular engineering of an alkaline naphthoquinone flow battery. *ACS Energy Lett.* **2019,** *4* (8), 1880-1887.

(18) Wang, C.; Yang, Z.; Wang, Y.; Zhao, P.; Yan, W.; Zhu, G.; Ma, L.; Yu, B.; Wang, L.; Li, G.; Liu, J.; Jin, Z., High-Performance Alkaline Organic Redox Flow Batteries Based on 2-Hydroxy-3-carboxy-1,4-naphthoquinone. *ACS Energy Lett.* **2018,** *3* (10), 2404-2409.

(19) Wedege, K.; Drazevic, E.; Konya, D.; Bentien, A., Organic Redox Species in Aqueous Flow Batteries: Redox Potentials, Chemical Stability and Solubility. *Sci Rep* **2016,** *6*, 39101.

(20) Zhang, W.; Soutrel, I.; Amrane, A.; Fourcade, F.; Geneste, F., Electrochemical processes coupled to a biological treatment for the removal of iodinated X-ray contrast media compounds. *Front. Chem.* **2020,** *8*, 646.

(21) Reber, D.; Thurston, J. R.; Becker, M.; Marshak, M. P., Stability of highly soluble ferrocyanides at neutral pH for energy-dense flow batteries. *Cell Reports Physical Science* **2023,** *4* (1).

(22) Guiheneuf, S.; Godet-Bar, T.; Fontmorin, J.-M.; Jourdin, C.; Floner, D.; Geneste, F., A new hydroxyanthraquinone derivative with a low and reversible capacity fading process as negolyte in alkaline aqueous redox flow batteries. *J. Power Sources* **2022,** *539*, 231600.

(23) Ozouf, I.; Fontmorin, J.-M.; Lebeuf, R.; Mathieu, G.; Guiheneuf, S.; Ozouf, G.; Nardello-Rataj, V.; Godet-Bar, T.; Floner, D.; Aubry, J.-M., Long-cycling of a water-soluble quinizarin derivative in redox flow batteries: Role of the cut-off voltage on the stability. *Electrochim. Acta* **2024,** *475*, 143570.

Graphic for manuscript